

We are IntechOpen, the world's leading publisher of Open Access books Built by scientists, for scientists

6,900

Open access books available

185,000

International authors and editors

200M

Downloads

Our authors are among the

154

Countries delivered to

TOP 1%

most cited scientists

12.2%

Contributors from top 500 universities



WEB OF SCIENCE™

Selection of our books indexed in the Book Citation Index
in Web of Science™ Core Collection (BKCI)

Interested in publishing with us?
Contact book.department@intechopen.com

Numbers displayed above are based on latest data collected.
For more information visit www.intechopen.com



Gamma Radiation in the Vicinity of the Entrance to Linac Radiotherapy Room

*Kinga Polaczek-Grelik, Aneta Kawa-Iwanicka,
Marek Rygielski and Łukasz Michalecki*

Abstract

Radiotherapy using high-energy photon beams (10–20 MV) is accompanied by the production of secondary neutron radiation via ($\gamma/X,n$) reactions. These interactions as well as subsequent neutron capture are the source of induced gamma radioactivity. When studied with standard range of spectrometric systems, only decay gamma radiation is usually registered, whereas a significant part of radiation—prompt gammas—is omitted, what might result in a significant underestimation of occupational risk for therapists in the vicinity of the door to the treatment room during therapeutic beam emission. Presented study has shown the main components of gamma radiation field in this localization investigated with the use of high-purity germanium spectrometry. Among them, prompt gamma radiation in light elements of concrete and in metal construction of the door, as well as 477.6 and 2224.6 keV photons emitted by neutron absorbing layers, contributes the most. Effective dose values depend on thickness of the door as well as on neutron production by particular linac and are within the range of 1.8–56.2 $\mu\text{Sv/h}$. Standard environmental radiometry could underestimate these values by about 60% due to low efficiency for high-energy photon counting.

Keywords: induced radioactivity, HPGe spectrometry, prompt gamma radiation, photon radiotherapy, radiation protection, occupational hazard

1. Introduction

Radiotherapy is one of the commonly used anticancer treatment methods, either applied alone or (what is more widely used) in conjunction with surgery and/or chemotherapy, as induction, supplement, or sensitizing agent. Therefore, it is administered as neoadjuvant, concurrent, or sequential (adjuvant) therapy [1–3]. In the first case, irradiation of a solid tumor may cause its shrinkage, making the subsequent surgery less extensive. In the second case, it is about to kill the cancer cell clusters too small to be seen and removed by the surgeon, limiting the risk of local recurrence or lymph node metastasis. The last issue is to gain the success of systemic chemotherapy, even in reducing treatment toxicity [1–3].

Generally, the distinction according to the localization of medically used radiation source relative to the patient's body divides radiotherapy into teletherapy—externally located radiation source, and internally located either sealed

(brachytherapy) or unsealed (nuclear medicine) radiation source in the form of radioactive nuclide. The use of external beams in radiotherapy (EBT) requires increased penetration of radiation to reach deeply located tumors sparing healthy tissues at the same time. Therefore, EBT generally employs higher energies of radiation, whereas brachytherapy benefits from limited range of ionizing radiation, which helps to spare healthy tissues neighboring the tumor region.

In the connection with the above, external beam radiotherapy is of higher concern in terms of radiological protection and safety work around ionizing radiation devices. Special attention is paid to the construction of the treatment room, what will be discussed later.

Every ionizing radiation type could be used for the purpose of radiotherapy and each of them has its advantages and disadvantages, making their availability and applicability common or restricted to a specific cases. Limited range of electrons in the tissue makes their use practical for shallow location of tumors, especially when healthy radiosensitive tissues are located close below/behind. On the other hand, forming uniform dose distribution with high target conformity is hardly to achieve using electron beams. Neutron beam production and guidance is a task difficult enough to limit the usage of fast neutron EBT, despite of lower oxygen enhancement ratio (OER—dependence of tumor cell sensitivity on its oxygenation) and entrance/surface dose in comparison with electron beams [4]. Photon beams in the form of Bremsstrahlung radiation produce similar shape of depth dose distribution as electron and neutron beams, showing regions of build-up, dose maximum, and quasiexponential decrease; however, skin sparing effect is more pronounced and radiation is more susceptible on shaping with the use of collimation/absorption blocks. The major advantage of using photons with energies of the order of MeV is the high penetration property. Therefore, using multiple directions of incident beam, it is possible to reach with therapeutic dose the tumor surrounded by healthy tissues from the outside. However, exit dose is not negligible and region of low doses due to scattered radiation is extended. In contrary, heavy charged particles give quite different dose distribution, follow the Bragg peak shape. It means that energy transfer in case of hadrons increases with decreasing their energy, just the opposite to neutral particles and electrons [4]. Moreover, high degree of tissue sparing is achieved at localizations beneath the tumor, since physical dose behind the peak tends to be negligible, what is of high beneficial when therapy concerns structures near radiation-sensitive organs. Among the biggest disadvantages, expensiveness of accelerator technology, unsure radiobiological and physical interactions of high-energy heavy charged particles in tissues are usually mentioned.

Despite the diverse advantages of every radiation type, radiotherapy with the use of electron and photon beams remains the most widespread and widely available technology. Modern techniques for accelerating electrons are both miniaturized and efficient, what enables to generate beams with a wide range of energies, from several keV to tens of MeV. However, the trend in radiotherapy is to replace electron beams with photon (X-ray) beams when employing dynamic, intensity, and volumetric modulated delivery of therapeutic dose distribution. Electrons are more easily controlled and accelerated in short sections than heavy charged particles and as such, linear electron accelerators for medical purpose are the most common once. Even nowadays, the development of devices producing X-ray beams for radiotherapeutic use is taking place, although rather in terms of increasing the number of degree of freedom in beam delivery than in terms of new method of beam producing and controlling. This development has led X-ray machines in radiotherapy from orthovoltage Roentgen machines through classical linacs to devices such as Tomotherapy[®] or CyberKnife[®]. Among them, only linear accelerators in their

classical form are designed to produce X-rays at accelerating potentials from a quite wide range (4–25 MV). This feature enables to clinically use highly penetrating X-ray beams with mean energies of 1–6 MeV with long tail of high-energy photons up to the end-point values of 4–25 MeV, respectively. Extensive comparison of linac beam spectra could be found in [5–10].

From physics point of view, variety of interactions of therapeutic beams with accelerator elements, room equipment, air and human body should be taken into account for two general reasons:

- precise planning of dose distribution in patient's body requires advanced dosimetric modeling of treatment unit and taking into account majority of ionizing radiation interaction types in terms of dose deposition, scattering, and density corrections [4];
- there is usually a need to limit the ionizing radiation field for radiation protection purposes, which should take into account secondary radiation generated by highly penetrative ionizing radiation.

The first one is crucial for radiotherapy beneficial outcome, whereas the second one is important as radiation safety issue. This second aspect is subjected in the present work studied with the use of gamma radiation spectrometry.

The most frequently used radiotherapy machine set in oncological center includes medical electron linear accelerator (linac), brachytherapy unit (usually high dose rate (HDR) type), and CT scanner with virtual simulation option for therapy positioning purposes. Usually, several linacs are installed to secure non-disturbance of radiotherapy process. From a radiation protection point of view, shielding vault should be designed with respect to the most penetrative radiation type among those used in particular room.

Several organizations have been releasing recommendations regarding shielding design and radiation safety issues since 1970s:

- National Council on Radiation Protection and Measurements (NCRP) [11–14];
- American Association of Physicists in Medicine (AAPM) [15, 16];
- International Atomic Energy Agency (IAEA) [17];
- Institute of Physics and Engineering in Medicine (IPeM) [18, 19];
- International Organization of Standards (ISO) [20];
- International Electrotechnical Commission (IEC) [21, 22].

German Industrial Norms (DIN) [23–26] also serve as practical reference worldwide. The relevant reports are constantly updating to include most recent development of radiotherapy machines as well as treatment techniques, e.g., the usage of photon energies above 10 MV, dual or even triple photon energy machines, intensity modulated radiation therapy (IMRT), stereotactic body radiation therapy (SBRT), or total body irradiation (TBI), which in comparison with static simple geometry fields require more radiation in terms of linac monitor units (MUs) to be emitted to deposit therapeutic dose in planning target volume (PTV) or usage of nonstandard field dimensions. New modalities in photon radiation therapy include also more complicated irradiation geometry, i.e., more incident beam directions

and thus, more complicated scattered radiation patterns (see: CyberKnife, Gamma Knife, or Tomotherapy).

Shielding considerations of medical linear accelerator room distinguish the following radiation groups, schematically presented in **Figure 1a**:

- primary beam—therapeutically useful radiation always directed to the linac isocenter (point of gantry rotation), what means when using rotational technique, this beam might incident on four out of six walls of treatment room;
- leakage radiation—ionizing radiation of the treatment beam type leaving the linac head through unattended ways—directed from the source (e.g., Bremsstrahlung conversion target) to outside; at the linac construction stage, it should be limited to a maximum of 0.2% and an average of 0.1% of the maximum absorbed dose [22] in $10 \times 10 \text{ cm}^2$ radiation field by, e.g., using beam stoppers or lead shielding;
- scattered radiation originating from the patient body, room walls, and equipment, directed in full solid angle, with wide range of energies.

The characteristic design of the therapeutic room, which is schematically presented in **Figure 1b**, meets the protective requirements against all of the above-mentioned radiation groups and contains:

- primary barrier, the thickest or made of concrete enriched with heavy material, e.g., barite;
- secondary barrier against leakage and scattered radiation, which is usually of lower intensity and/or energy than primary beam; therefore, the barrier is thinner than the primary barrier;
- maze, as a construction protecting the entrance from direct incidence of unattenuated beam, with the purpose of lengthening the scattering radiation path.

The use of high-energy radiotherapeutic beams ($E > 10 \text{ MeV}$) is additionally accompanied by the aspect of generation of secondary radiation, which will be widely addressed below.

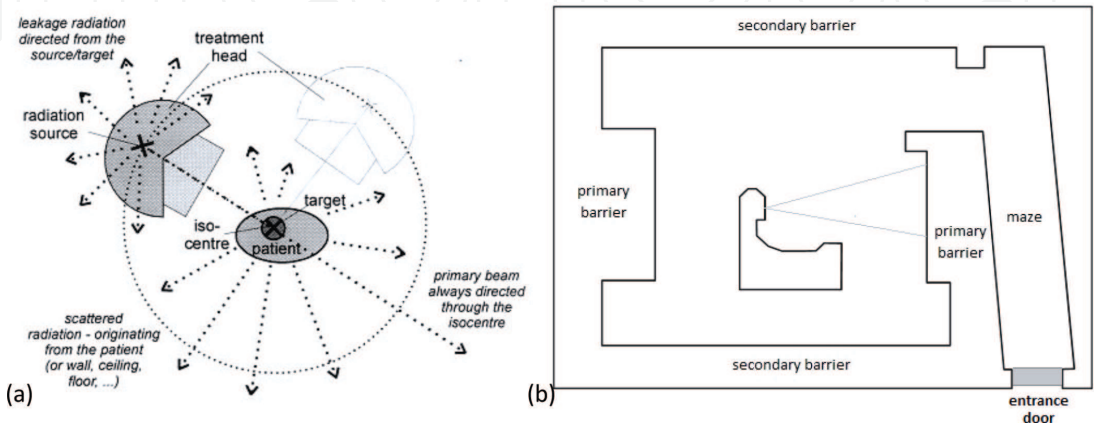


Figure 1.
(a) Schematic presentation of different radiation groups the linac room shielding must face with, available from [27]; (b) scheme of typical radiotherapy treatment vault. Medical accelerator head is able to rotationally move on 360° around the axis perpendicular to the beam (gray-line cone) central axis. The entrance door as the localization relevant for the presented study is also marked.

Radiotherapeutic photon beams in the form of Bremsstrahlung radiation generated on conversion target by electrons accelerated at potentials of the order of MV have wide-energy spectrum up to energy determined by the nominal accelerating potential used. Therefore, in high-energy therapeutic beam (10–20 MV) even up to about 20% of photons could have energies above 8 MeV, which is the approximate threshold energy for photonuclear reactions. However, for tungsten (the main component of linac collimation system)—nuclear photo effect starts approximately from 5 MeV. Generally, the higher mass number of nuclide, the lower threshold energy, and for defined energy—the higher cross section for photon absorption by the nucleus is observed, what is presented in **Figure 2**. Among the products of such reactions are secondary gamma rays (when inelastic scattering occurs) or nucleons (protons, neutrons, or their groups: deuterons, alphas), when a reaction through a stage of compound nucleus has occurred. The final nucleus either nucleon-deficient (photonuclear reaction product) or nucleon-excess (neutron absorption product) could be unstable and undergo radioactive decay. From occupational radiation protection point of view, high-penetrative radiation, i.e., prompt and decay gamma rays as well as neutrons are of importance, since (1) they are able to reach entrance to the treatment room, (2) they form a significant part of radiation leakage from the treatment room through the door.

The energy range of photons and electrons used in linac radiotherapy is sufficient to trigger a nuclear reaction via $(\gamma/X,n)$, $(\gamma/X,p)$, and $(e,e'n)$ mechanisms and to observe subsequent nuclear reactions of secondary generated particles, among

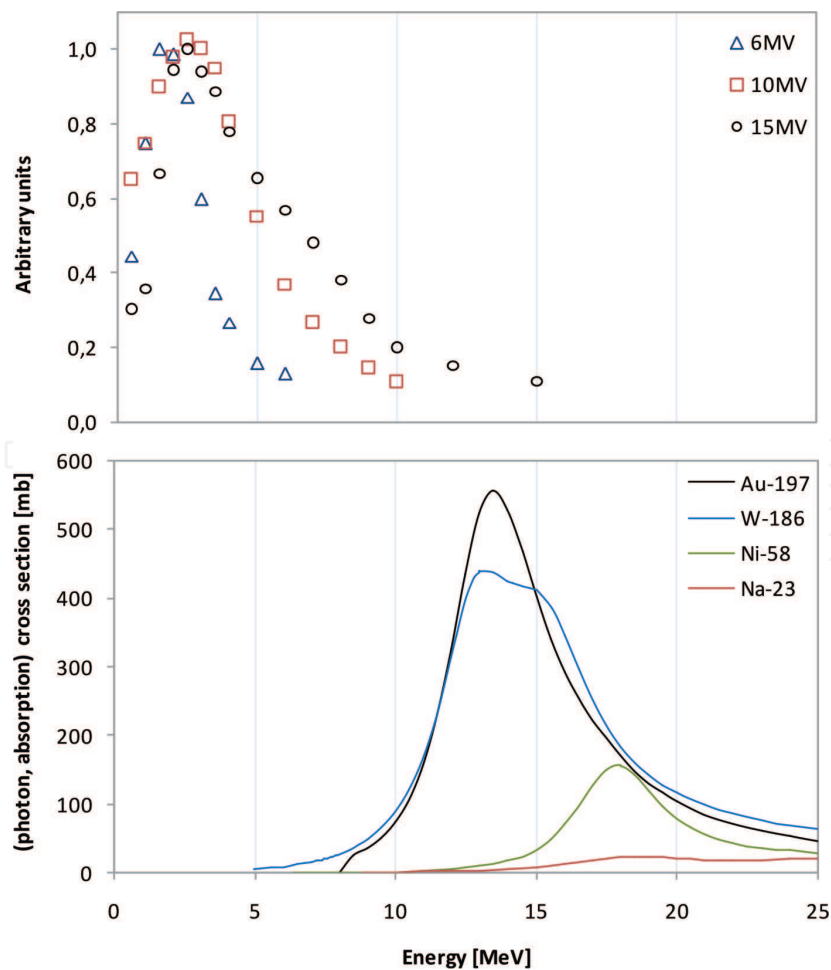


Figure 2.
The comparison of photon beam spectra (modeled by us in commercial dose verification system) with cross sections of photon absorption nuclear reactions [28] for commonly observed activation target nuclides, in terms of energy overlapping regions.

which $(n,n'\gamma)$ and (n,γ) are the most commonly observed, for fast and thermalized neutrons, respectively. Every mechanism mentioned above could activate radionuclides. Nevertheless, the majority of induced radioactivity is found in construction materials of the accelerator head, mostly in heavy elements of collimation and beam shaping system. The contribution of particular elements of linac head in overall induced radioactivity is studied mostly with Monte Carlo simulations, as in: [29, 30]. However, gamma radiation spectrometry is a good tool for identification of particular radionuclides and their contribution in this phenomenon, for example, see: [31]. The apparent linac radioactivity depends on the localization of measuring point; therefore, the radiation hazard due to this phenomenon is different for patients and for the staff, with the dominant contribution of tungsten collimator or head casing, respectively [32]. Induced radioactivity has been also observed and investigated in tissues [33–36], air [37], treatment couch [38], and treatment accessories stored inside the linac room [39]. Moreover, the dependence of induced activity on the therapeutic dose rate could be observed in some cases, i.e., when half-life of radioisotope is comparable with the time of beam emission, and is more pronounced for higher nominal accelerating potentials [35].

Among the mechanisms of radionuclide activation outside the field of irradiation, neutron capture contributes the most. Linacs used nowadays are not routinely equipped with shielding constructions dedicated for neutrons; therefore, neutron fluence all over the treatment room is reported [32, 40–44] in the amount sufficient for inducing radioactivity at measurable level. Therefore, medical linear accelerators are often characterized in terms of neutron source strength Q [14, 44], which depends on beam nominal potential, as presented in **Figure 3**.

The spectrum of neutron flux undergoes changes via scattering mechanisms. Leaving the linac head, the mean energy of neutrons is of the order of 1 MeV, on treatment couch, an additional peak at thermal energies is already observed and neutrons impinging the door have an average energy of ~ 0.2 MeV [45, 46].

Neutron radiation weighting factor for effective dose calculation strongly depends on energy, having maximal values around 1 MeV [47]. The cross section of (n,γ) nuclear reaction follows the $1/E$ dependence with some resonance peaks at intermediate energies [28]. Therefore, high-energy neutrons contribute mostly to the dose, whereas slow neutrons to the phenomenon of induced radioactivity.

It is of high importance to be aware of the physical mechanisms of radiation absorption and removal from the beam. These are in principle different for various radiation types. Nevertheless, similar mechanisms might be observed for various radiation types but occurring with different efficiency.

The readily used in diagnostic radiology heavy metal shielding is no longer valid in high-energy radiotherapy rooms due to the generation of secondary

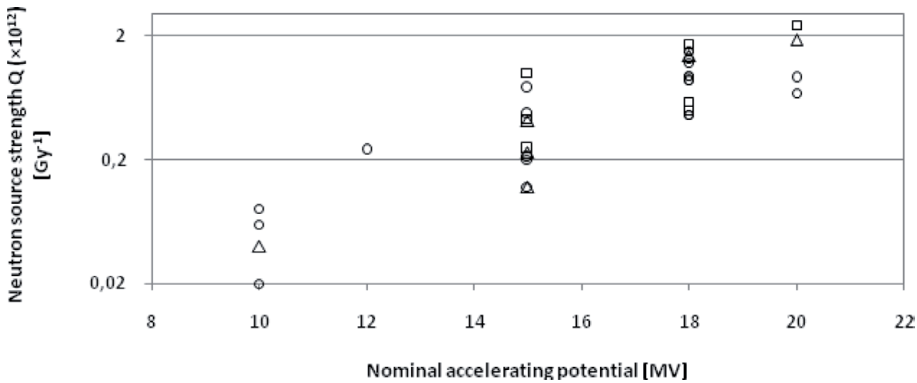


Figure 3. The comparison of neutron source strength values reported in [14] (o), [44] (□), and obtained by us (Δ).

radiation via nuclear reactions, as discussed above. Therefore, concrete, barite-concrete, earth bricks, and similar materials are preferred during solid shielding construction. These, built of mostly light elements, for which neutron production threshold energies are relatively high, i.e., tens of MeV, should not gain the production of secondary radiation. Additional lamination of maze walls as well as using multibend geometries are the solutions advised for increasing the neutron absorption before reaching the entrance. These solutions help to slim down the room door or even built the door-less entrance, minimizing secondary radiation at the entrance [48]. Typical door construction contains the most inner layer of neutron-absorption material (polyethylene, paraffin, or borax), enclosed with heavy photon-absorption layer (lead, tungsten) coated with industrial material, typically of stainless steel or wood. Unfortunately, to maintain an acceptable mechanics/kinetics of the door, the weakness of this radiation barrier must be accepted. Therefore, from radiation protection point of view, the vicinity of entrance to the treatment room is not an advised place for staying during radiotherapy beam emission as a location with increased occupational radiation hazard. The standard radiometric methods used in such case could seriously underestimate the radiation indications since they are calibrated on ^{60}Co or ^{137}Cs sources. Although average energy of leakage/scattered radiation reaching the entrance door is close to the energies of these radionuclide sources, prompt gamma rays produced during neutron capture are much more energetic (over a dozen of MeV), therefore, detected with very low efficiency by these devices. Moreover, standard spectrometric range of detected energies is aimed at measuring decay gamma rays up to about 3 MeV and therefore omits significant range of prompt gammas. That is the reason which makes gamma spectrometry with extended energy range to be adequate for more precise investigation of the occupational radiation hazard near the entrance door to the high-energy medical linac room.

2. Semiconductor spectrometry and its application for radiation characterization

Semiconductor high-purity germanium (HPGe) detectors are most suitable for the investigation of gamma radiation spectra of unknown origin since the excellent energy resolution enables the exact identification of any radionuclide, which contributes to the radiation field in measured localization. Their use is, however, limited due to the need of liquid nitrogen cooling; therefore, scintillation or room-temperature semiconductor detectors, both with limited resolution, are used instead.

The spectrometric system used in this study, as shown in **Figure 4**, consists of:

- coaxial HPGe detector with reversed electrodes (ReGe), manufactured by Canberra Inc., having 40% relative efficiency and characterized by the resolution of 2.1 keV FWHM @ 1332 keV; the use of a standard spectrometric gain of 5.0 enables for spectra registration up to 3.2 MeV;
- InSpector™ 2000 MultiChannel Analyzer (MCA) with 8194 channels;
- Genie™ 2000 v.3.2.1 Gamma Acquisition and Analysis Software (Canberra Inc.).

The carbon-composite entrance window enables the registration of low-energy photons (above 7 keV). The end-point energy of measured spectra has been set

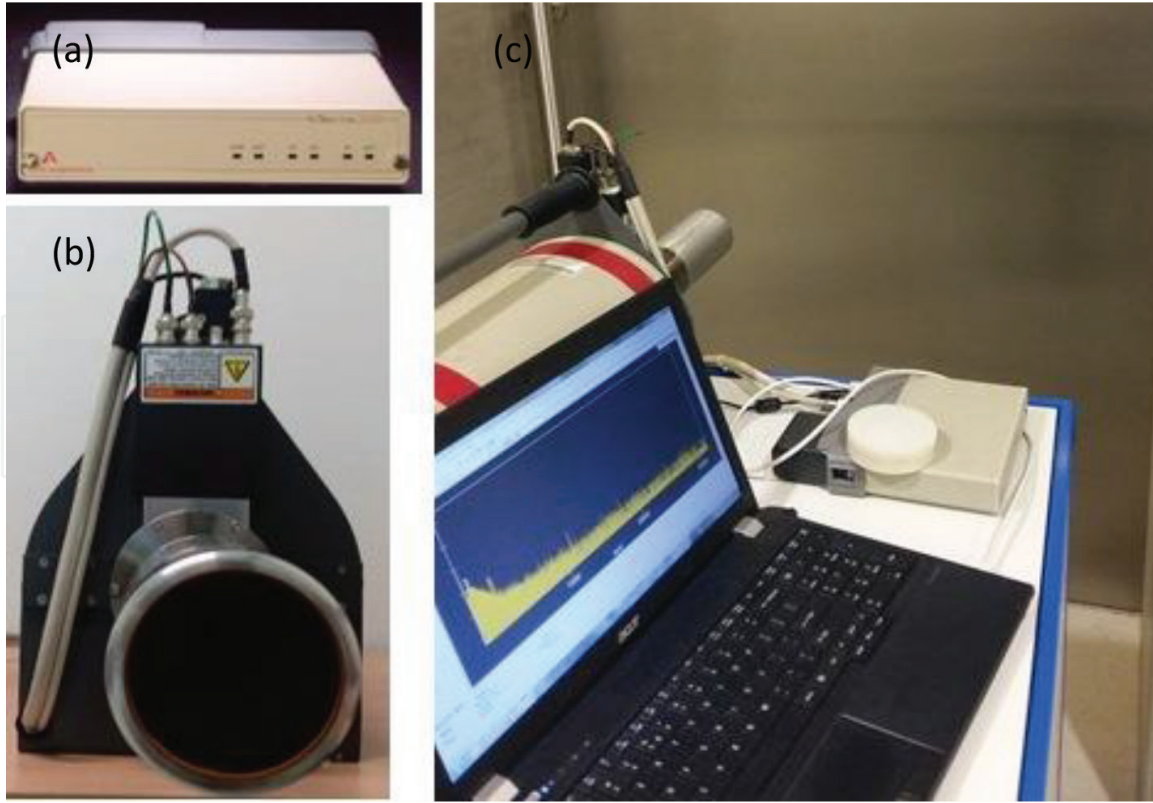


Figure 4. ReGe gamma spectrometer used in present study: (a) multichannel analyzer, (b) front view of high-purity germanium detector with carbon-composite entrance window, and (c) measurement configuration 50 cm from the entrance door to the linac radiotherapy room.

by adjusting the gain value of MCA. This enables for spectra registration up to the energy of 3–10 MeV.

Energy calibration of spectrometric system has been performed for standard MCA gain (5.0) with the use of radioisotope sealed sources (1 cm Ø) having activity of the order of 10 kBq. Subsequently, it was checked that the calibration scales linearly inversely with the spectrometric gain.

Spectrometric efficiency has been modeled in In Situ Object Counting Software (ISOCS™, Canberra Inc.), applying full factory characterization of a given detector performed with the use of NIST-traceable sources and MCNP Monte Carlo modeling code, supplied by the manufacturer. The geometry of rectangular complex plane for calculating the detection efficiency has been chosen from the ISOCS predefined templates as best matching to the experimental conditions, giving the possibility to include the multilayer design of the entrance door. The energy-dependent photon detection efficiency (ϵ) of spectrometric system has been finally described with the following function:

$\ln(\epsilon) = a + b \cdot \ln(E) + c \cdot \ln(E)^2 + d \cdot \ln(E)^3 + e \cdot \ln(E)^4 + f \cdot \ln(E)^5$, with the fitting parameters of a–f.

The analysis of registered spectra (photopeaks' identification and net areas counting) has been performed using unidentified second differential and nonlinear LSQ fit in Genie™ 2000 software. The sources of gamma radiation (activated nuclides) have been identified on the base of photopeaks' energies, whereas areas under these photopeaks were used for photon flux density (Φ) assessment on the basis of Eq. (1), for a defined detector front surface (S_{Ge}) and life time (LT) of each measurement.

$$\Phi(E) [cm^{-2}s^{-1}] = \frac{Peak_net_area(E)}{\epsilon(E) \cdot S_{Ge}[cm^2] \cdot LT[s]} \quad (1)$$

The recommended quantity for the purpose of limitation of ionizing radiation exposure is the effective dose (E_d). However, radiation protection and operational quantities are distinguished according to the relevance to radiation health effects and possibility to be measured, respectively. These are presented in reports 26, 60, and 103 of International Commission on Radiological Protection (ICRP) and in reports 66 and 85 of International Commission on Radiation Units and Measurements (ICRU) [47, 49–52]. Moreover, conversion coefficients of radiation fluence to organ absorbed doses as well as equivalent doses and effective dose are also supplied in ICRP 74 and 116 as well as in ICRU 57 reports [53–55]. This enables the risk estimation on the basis of different measuring quantities.

3. Results and discussion

Gamma radiation spectrometry system was placed 50 cm in front of linac treatment room entrance door, at the height of 1 m above the floor (see **Figure 4**), at a localization representative for dose rate assessment for the staff waiting for the end of patient irradiation.

The spectra were registered during emission of 6–18 MV photon beams with a dose rate of 450 MU/min. The gantry angle of 90 or 270° and irradiation field size of 40 × 40 cm² were set to achieve maximal intensity of radiation reaching the entrance door, to study the worst scenario of occupational hazard.

3.1 Comparison of spectra for various beam energies

The detailed characteristics of gamma ray spectra acquired in standard and extended energy range near the linac room door are presented in **Table 1**. The energies of photons in 6 MV beam are too low to trigger nuclear reactions; therefore, induced radionuclides are not observed on the spectrum outside the door in this case, as shown in **Figure 5**. Nevertheless, the increase in low-energy continuous part of the registered spectrum in comparison with natural background radiation indicates that part of scattered radiation from therapeutic beam penetrates the door.

Spectra registered during high-energy beam emission (10–18 MV), as shown in **Figure 5**, are dominated by two processes: positron creation, since annihilation peak at 511 keV is clearly visible, and neutron capture in hydrogen-rich material inside the door, due to the presence of a peak at 2224.6 keV, which is the neutron-binding energy in deuterium nucleus. The intensity of these processes could be correlated not only with neutron source strength of particular linac working at defined accelerating potential, but also with the amount of hydrogen-rich material used in door construction. The peak at 477.6 keV is due to the presence of boron (mostly in the form of borax–sodium tetraborate decahydrate) and is a consequence of $^{10}\text{B}(n,\alpha)^7\text{Li}$ reaction, where 477.6 keV is the deexcitation energy of lithium nucleus. The broadening of this peak has Doppler effect—origin, widely discussed in [56]. Since door construction is not unified and the usage of paraffin/polyethylene (as hydrogen-rich materials) or borax as neutron absorption agents depends on the construction concept, the intensity of the 477.6 keV line should not be directly connected with the therapeutic beam energy (see **Figure 5**: 15 MV vs. 18 MV cases) or even may not occur at all, whereas hydrogen capture of neutron is present for all linacs studied by us.

The gamma ray spectra are dominated by the abovementioned interactions; however, the minor contributions come from:

- $(n,n'\gamma)$ and (n,γ) interactions in germanium crystal of HPGe spectrometer, which proves that neutrons contribute to the door-leakage radiation outside the treatment room;

Source	Origin	Photon energy [keV]
Germanium detector	$^{72}\text{Ge}(\text{n},\gamma)^{73\text{m}}\text{Ge}$	66.7
	$^{74}\text{Ge}(\text{n},\gamma)^{75\text{m}}\text{Ge}$	139.7
	$^{70}\text{Ge}(\text{n},\gamma)^{71\text{m}}\text{Ge}$	174.9; 198.4; 499.9
	$^{73}\text{Ge}(\text{n},\gamma)^{74}\text{Ge}^*$	595.9
	$^{74}\text{Ge}(\text{n},\text{n}'\gamma)$	595.9; 608.3; 867.9; 1204.2
	$^{72}\text{Ge}(\text{n},\text{n}'\gamma)$	689.6
Metal elements of door construction	$^{56}\text{Fe}(\text{n},\gamma),$ $^{54}\text{Fe}(\text{n},\gamma)$	352.4; 7631.1; 7645.5
	$^{56}\text{Fe}(\text{n},\gamma)$	570.0; 810.6; 920.5; 1019.0; 1358.6; 1612.8; 1358.6; 1725.3; 1972.3; 2129.2; 2425.7; 2469.2; 2526.5; 2721.3; 3185.2; 3436.6; 3854.3; 4218.3; 4406.1; 5357.4; 5920.4; 6018.5; 7278.8; 7631.1; 7645.5; 9297.7
	$^{27}\text{Al}(\text{n},\gamma)^{28}\text{Al}$	1779.0; 3033.9
	$^{12}\text{C}(\text{n},\gamma)$	1261.8; 4945.3
Shielding elements of door construction	$^1\text{H}(\text{n},\gamma)$	2224.6
	$^{10}\text{B}(\text{n},\alpha)^7\text{Li}$	477.6
	$^{207}\text{Pb}(\text{n},\gamma)$	7367.8
Concrete	$^{39}\text{K}(\text{n},\gamma)$	770.3;
	$^{35}\text{Cl}(\text{n},\gamma)$	516.7; 575.8; 1164.9; 1951.1; 1959.3; 2863.8; 2876.9; 3061.8; 3195.4; 4082.8; 4298.6; 4979.9; 5204.5; 6110.8; 6619.6; 6627.8; 7414.0; 7790.3
	$^{40}\text{Ca}(\text{n},\gamma)$	707.7; 1942.7; 2001.3; 3610.2; 4418.5; 6419.6
	$^{23}\text{Na}(\text{n},\gamma)$	834.7; 2517.8
	$^{28}\text{Si}(\text{n},\gamma)$	1273.3; 2092.9; 3101.8; 3539.0; 3723.1; 4933.9; 6379.8
	$^{24}\text{Mg}(\text{n},\gamma)$	3413.1; 3916.8
	$^{31}\text{P}(\text{n},\gamma)$	3899.9

Table 1.
Characteristics of gamma ray spectra registered in the energy range of 10 keV–10 MeV near the door to linac therapy room during emission of 10–18 MV photon beams.

- (n,γ) reactions in concrete elements: ^{23}Na , ^{24}Mg , ^{28}Si , ^{31}P , ^{35}Cl , ^{39}K , ^{40}Ca ;
- (n,γ) reactions in metals: ^{27}Al and ^{56}Fe .

Neutron capture nuclear reaction is accompanied by prompt gamma rays but also decay gamma radiation might be observed, when originated nucleus is radioactive. The first mentioned radiation type is observed only during emission of high-energy therapeutic beam, but observed energies are mostly above 2 MeV, whereas the second group of gammas has energies up to about 2 MeV and contributes to the increased background after the end of therapeutic beam emission, with a characteristic half-life.

Spectra registered in extended energy range prove that neutron capture process on light elements (mainly concrete) occurs intensively. The main differences between linac room shielding properties from occupational hazard point of view (for defined therapeutic beam) are due to the diverse construction of the door and specific material used, for example: borated polyethylene or paraffin alone will result in the presence of 477.6 keV line or not, which will affect the intensity of

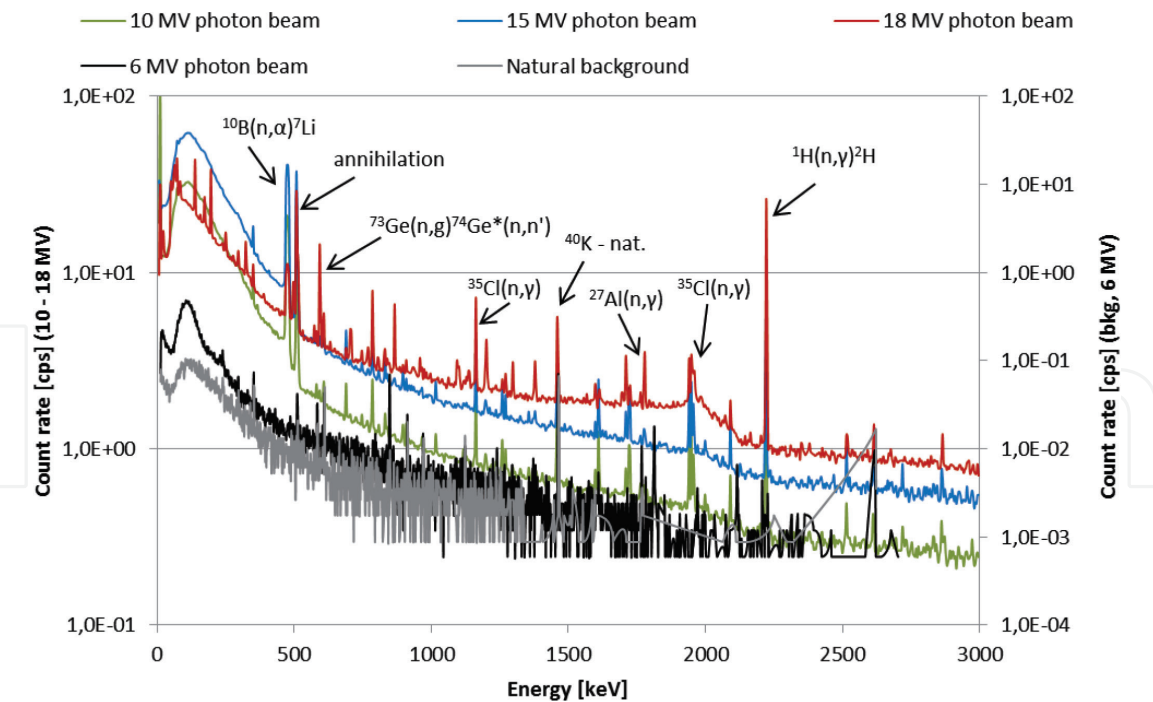


Figure 5.
The comparison of spectra registered behind the treatment room door during emission of linac photon beams. Natural background radiation is presented for reference. Only the most intense lines (mentioned in the text above) are marked for clarity of presentation. Detailed analysis is presented in **Table 1**.

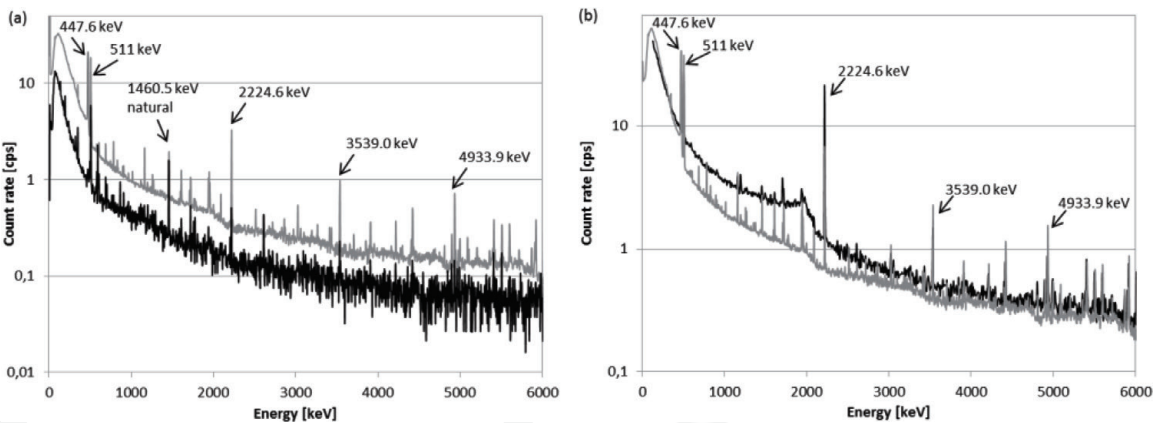


Figure 6.
Comparison of spectra registered for (a) 10 MV photon beams and (b) 15 MV photon beams, when thick (black line) and thin (gray line) door constructions are used. (See text above for the explanation of differences.)

2224.6 keV line. The comparison of spectra presented in **Figure 6** demonstrates the differences between thick and thin door constructions designed for (a) higher beam energy than currently used and (b) maximum beam currently in use.

3.2 Spectrometry—Based dose assessment

In the present study, the effective dose in front of linac room entrance door has been estimated on the base of photon flux density obtained according to the Eq. (1) and using conversion coefficients for AP geometry given in ICRP report 116 [54]. Specific values of these coefficients for energies registered on gamma ray spectra were calculated using Lagrange interpolation formula of third degree. The average total uncertainty of calculated effective dose values of 25% includes the accuracy of conversion coefficients as well as the uncertainty of photopeaks' area determination at the registered spectra.

Effective doses in studied location depend on the neutron source strength Q of particular linac as well as on the construction of the treatment room door. For 18-MV photon beam, more important is the first factor (linac construction), ranging the doses from 30.6 ± 7.7 to 56.2 ± 14.1 $\mu\text{Sv/h}$. The second factor plays the crucial role for 10 MV photon beams, for which neutron generation is of the lowest intensity, ranging the doses from 1.8 ± 0.4 $\mu\text{Sv/h}$ (for flattening filter-free (FFF) beam), through 3.4 ± 0.8 $\mu\text{Sv/h}$ (for thick door construction) up to 10.5 ± 2.6 $\mu\text{Sv/h}$ (for thin door construction). However, also in this case, neutron production intensity in linac head plays significant role, what is concluded from the differences between FFF beam and conventional linac, since flattening filter takes part in neutron production [29, 30]. Effective dose rates measured during 15-MV beam emission using Geiger-Mueller radiometer (calibrated on ^{60}Co source) and the result obtained using spectrometry analysis presented here are 13.5 ± 3.0 $\mu\text{Sv/h}$ and 22.2 ± 5.5 $\mu\text{Sv/h}$, respectively. This comparison shows that even 60% of dose could be omitted in the first case when excluding high-energy component of radiation leakage through the door due to prompt gamma rays accompanying the neutron capture process.

Production of neutron secondary radiation during emission of high-energy photon therapeutic beams is generally known and widely studied issue [29–46, 48]. Also, the phenomenon of high-energy X-rays and secondary neutron-induced radioactivity is well recognized [57]. However, the impact of photon radiation connected with neutron interaction in treatment room shielding materials on occupational safety is still difficult to assess experimentally in clinical conditions due to limited availability of high-resolution extended-energy range spectrometry systems, which often require special operating conditions (e.g., nitrogen cooling) and time-/labor-consuming data analysis. Nevertheless, recommendations concerning design of linac rooms [17] refer to publications devoted to this issue [58]. The use of a spectrometer (the usefulness of which has been demonstrated in presented study) is advised by IAEA [59] as a supplementary method for workplace monitoring, and its usage to characterize the energy spectrum of a given radiation type is recommended to support the performance of routinely used monitoring instruments.

4. Conclusion

The qualitative analysis performed by us has shown that the major component of gamma radiation field near the treatment room door comes from prompt photons emitted during neutron capture reaction and is common in door construction as well as in concrete materials. Comprehensive study of this issue requires extended energy range of spectrometric system, as demonstrated in presented investigations. High-energy gamma rays above 3 MeV (omitted in standard spectrometric measurements) contribute to the effective dose values from 26 to 58%, for low (10 MV FFF beam) and for high (18 MV beam) neutron source strength linacs, respectively.

Reactions intended for neutron capture in door construction: $^{10}\text{B}(n,\alpha)^7\text{Li}$ and $^1\text{H}(n,\gamma)^2\text{H}$ contribute to the effective dose of 0–17% and 4–19%, respectively. Borated inner layer of the door is not always used, whereas hydrogen-rich material is the commonly used neutron absorber.

Presented study proves the correctness of radiation protection guidelines to avoid the vicinity of treatment door during therapeutic beam emission and additionally provides the justification in terms of dose values and mechanisms of gamma ray production.

Acknowledgements

This work was possible due to one of the authors (KPG) involvement in scientific activity in University of Silesia in Katowice, Poland. Therefore, the authors express their gratitude for the opportunity to use in situ gamma spectrometric system.

Conflict of interest

The authors certify that they have no affiliations with or involvement in any organization or entity with any interest in the subject matter or materials discussed in this manuscript.

Author details

Kinga Polaczek-Grelík^{1*}, Aneta Kawa-Iwanicka¹, Marek Rygielski²
and Łukasz Michalecki¹

¹ Nu-Med Cancer Diagnosis and Treatment Centre, Katowice, Poland

² Nu-Med Cancer Diagnosis and Treatment Centre, Tomaszów Mazowiecki, Poland

*Address all correspondence to: kinga.polaczek-grelik@nu-med.pl

IntechOpen

© 2019 The Author(s). Licensee IntechOpen. This chapter is distributed under the terms of the Creative Commons Attribution License (<http://creativecommons.org/licenses/by/3.0>), which permits unrestricted use, distribution, and reproduction in any medium, provided the original work is properly cited. 

References

- [1] Glatzer M, Elicin O, Ramella S, Nestle U, Putora PM. Radio(chemo) therapy in locally advanced non small cell lung cancer. *European Respiratory Review*. 2016;**25**:65-70. DOI: 10.1183/16000617.0053-2015
- [2] Joiner M, van der Kogel A, editors. *Basic Clinical Radiobiology*. 4th ed. London: Hodder Arnold; 2009. p. 391
- [3] Sas-Korczynska B, Sokolowski A, Korzeniowski S. The influence of time of radio-chemotherapy and other therapeutic factors on treatment results in patients with limited disease small cell lung cancer. *Lung Cancer*. 2013;**79**:14-19. DOI: 10.1016/j.lungcan.2012.10.004
- [4] Podgorsak EB. *Radiation Physics for Medical Physicists*. 1st ed. Berlin Heidelberg: Springer-Verlag; 2006. p. 437. DOI: 10.1007/978-3-642-008745-7
- [5] Desobry GE, Boyer AL. Bremsstrahlung review: An analysis of the Schiff spectrum. *Medical Physics*. 1991;**18**(3):497-505. DOI: 10.1118/1.596653
- [6] Rogers DWO, Faddegon BA, Ding GX, Ma C-M, BEAM WJ. A Monte Carlo code to simulate radiotherapy treatment unit. *Medical Physics*. 1995;**22**(5):503-524. DOI: 0094-2405/95/22(5)/503/22
- [7] Sheikh-Bagheri D, Rogers DWO. Sensitivity of megavoltage photon beam Monte Carlo simulations to electron beam and other parameters. *Medical Physics*. 2002;**29**(3):379-390. DOI: 10.1118/1.1445413
- [8] Sheikh-Bagheri D, Rogers DWO. Monte Carlo calculation of nine megavoltage photon beam spectra using the BEAM code. *Medical Physics*. 2002;**29**(3):391-402. DOI: 10.1118/1.1446109
- [9] Ali ESM, Rogers DWO. An improved physics—Based approach for unfolding megavoltage bremsstrahlung spectra using transmission analysis. *Medical Physics*. 2012;**39**(3):1663-1675. DOI: 10.1118/1.3687164
- [10] Ali ESM, Rogers DWO. Functional forms for photon spectra of clinical linacs. *Physics in Medicine and Biology*. 2012;**57**(1):31-50. DOI: 10.1088/0031-9155/57/1/31
- [11] NCRP Report 49. *Structural Shielding Design and Evaluation for Medical Use of X Rays and Gamma Rays of Energies Up to 10 MeV*. 1976
- [12] NCRP Report 147. *Structural Shielding Design for Medical X-Ray Imaging Facilities*. 2004
- [13] NCRP Report 144. *Radiation Protection for Particle Accelerator Facilities*. 2003
- [14] NCRP Report 151. *Structural Shielding Design and Evaluation for Megavoltage X and Gamma-Ray Radiotherapy Facilities*. 2005
- [15] AAPM 19. *Neutron Measurements Around High Energy X-Ray Radiotherapy Machines*. 1986. p. 36
- [16] AAPM 108. *PET and PET/CT Shielding Requirements*. 2003. p. 12. DOI: 10.1118/1.2135911
- [17] IAEA Safety Reports Series, No 47. *Radiation Protection in the Design of Radiotherapy Facilities*. 2006. p. 129
- [18] IPEM Report 75. *Design of Radiotherapy Treatment Room Facilities*. 1997. p. 304. DOI: 10.1088/978-0-7503-1440-4
- [19] IPEM Reports. 2018. Available from: <https://www.ipem.ac.uk/ScientificJournalsPublications/>

- IPEMReportSeries/
 AvailablePublications.aspx. [Accessed:
 04-11-2018]
- [20] ISO 16645. Radiological Protection—Medical Electron Accelerators—Requirements and Recommendations for Shielding Design and Evaluation. 2016. p. 84
- [21] IEC 60976. Medical Electrical Equipment—Medical Electron Accelerators—Functional Performance Characteristics. 2007. p. 172
- [22] IEC 60601-2-1. Medical Electrical Equipment—Part 2-1: Particular Requirements for the Basic Safety and Essential Performance of Electron Accelerators in the Range 1 MeV to 50 MeV. 2014. p. 134
- [23] DIN EN 60601-2-1. Particular Requirements for the Basic Safety and Essential Performance of Electron Accelerators in the Range 1 MeV to 50 MeV. 2015
- [24] DIN 6812:2013-06. Medical X-Ray Equipment up to 300 kV—Rules of Construction for Structural Radiation Protection. 2013. p. 43
- [25] DIN 6847-2:2014-03. Medical Electron Accelerators—Part 2: Rules for Construction of Structural Radiation Protection. 2014. p. 48
- [26] DIN 6875-20:2016-08. Special Radiotherapy Equipments—Part 20: Proton Therapy—Rules for Construction of Structural Radiation Protection. 2016
- [27] IAEA Training Material on Radiation Protection in Radiotherapy [Internet]. 2018. Available from: <https://www.iaea.org/resources/rpop> [Accessed: 04-11-2018]
- [28] National Nuclear Data Center. Sigma Evaluated Nuclear Data File (ENDF) Retrieval & Plotting [Internet]. Available from: <https://www.nndc>
- bnl.gov/sigma/search.jsp [Accessed: 09-11-2018]
- [29] Pena J, Franco L, Gomez F, Iglesias A, Pardo J, Pombar M. Monte Carlo study of siemens primus photoneutron production. *Physics in Medicine and Biology*. 2005;**50**:5921-5933. DOI: 10.1088/0031-9155/50/24/011
- [30] Becker J, Brunckhorst E, Schmidt R. Photoneutron production of a Siemens primus linear accelerator study by Monte Carlo methods and a paired magnesium and boron coated magnesium ionization chamber system. *Physics in Medicine and Biology*. 2007;**52**:6375-6387. DOI: 10.1088/0031-9155/52/21/002
- [31] Polaczek-Grelík K, Karaczyn B, Konefal A. Nuclear reactions in linear medical accelerators and their exposure consequences. *Applied Radiation and Isotopes*. 2012;**70**:2332-2339. DOI: 10.1016/j.apradiso.2012.06.021
- [32] Janiszewska M, Polaczek-Grelík K, Raczkowski M, Szafron B, Konefal A, Zipper W. Secondary radiation dose during high-energy total body irradiation. *Strahlentherapie und Onkologie*. 2014;**190**(5):459-466. DOI: 10.1007/s00066-014-0635-z
- [33] Gudowska I, Brahme A, Andreo P, Gudowski W, Kierkegaard J. Calculation of absorbed dose and biological effectiveness from photonuclear reactions in a bremsstrahlung beam of end point 50 MeV. *Physics in Medicine and Biology*. 1999;**44**(9):2099-2125
- [34] Allen PD, Chaudhri MA. Charged photoparticle production in tissue during radiotherapy. *Medical Physics*. 1997;**24**(6):837-839
- [35] Polaczek-Grelík K, Orlef A, Dybek M, Konefal A, Zipper W. Linear accelerator therapeutic dose—Induced radioactivity dependence. *Applied Radiation and Isotopes*.

2010;**68**(4-5):763-766. DOI: 10.1016/j.apradiso.2009.09.051

[36] Polaczek-Grelík K, Konefal A, Orlef A, Zipper W. Radioactivity induced in bones during radiotherapy treatment with the use of 20 MV accelerator beam. Polish Journal of Environmental Studies. 2006;**15**(1A):195-197

[37] McGinley PH. Air activation produced by high-energy medical accelerators. Medical Physics. 1983;**10**(6):796-800. DOI: 10.1118/1.595358

[38] Rawlinson JA, Islam MK, Galbraith DM. Dose to radiation therapists from activation at high-energy accelerators used for conventional and intensity-modulated radiation therapy. Medical Physics. 2002;**29**:598-608. DOI: 10.1118/1.1463063

[39] Konefal A, Orlef A, Dybek M, Maniakowski Z, Polaczek-Grelík K, Zipper W. Correlation between radioactivity induced inside the treatment room and the undesirable thermal and resonance neutron radiation produced by linacs. Physica Medica. 2008;**24**:212-218. DOI: 10.1016/j.ejmp.2008.01.014

[40] Polaczek-Grelík K, Karaczyn B, Grządziel M, Pieńkos M, Konefal A, Zipper W. The map of thermal and resonance neutron distribution inside the treatment room for accelerator therapy. In: Drzazga Z, Slosarek K, editors. Some aspects of medical physics – *In Vivo* and *In Vitro* Studies – Series of Monograph Polish Journal of Environmental Studies. Olsztyn, Poland: HARD; 2010. pp. 139-145

[41] Vega-Carrillo HR, Manzanares-Acuna E, Iniguez MP, Gallego E, Lorente A. Study of room-returned neutrons. Radiation Measurements. 2007;**42**:413-419. DOI: 10.1016/j.radmeas.2007.01.036

[42] Konefal A, Orlef A, Laciak M, Ciba A, Szewczuk M. Thermal and resonance neutrons generated by various electron and X ray therapeutic beams from medical linacs installed in Polish oncological centers. Reports of Practical Oncology and Radiotherapy. 2012;**17**(6):339-346. DOI: 10.1016/j.rpor.2012.06.004

[43] Martinez Ovalle SM. Neutron dose equivalent in tissue due to linacs of clinical use. In: Kataria T, editor. Frontiers in Radiation Oncology. Rijeka, Croatia: InTech; 2013. pp. 91-112. DOI: 10.5772/3065

[44] Howell RM, Kry SF, Burgett E, Hertel NE, Followill DS. Secondary neutron spectra from modern Varian, Siemens and Elekta linacs with multileaf collimators. Medical Physics. 2009;**36**(9):4027-4038. DOI: 10.1118/1.3159300

[45] Banuelos-Frias A, Borja-Hernandez CG, Guzman-Garcia KA, Valero-Luna C, Hernandez-Davila VM, Vega-Carrillo HR. Neutron spectra and $H^*(10)$ of photoneutrons inside the vault room of an 18 MV linac. Revista Mexicana de Fisica. 2012;**58**:192-194

[46] Kralik M, Turek K. Characterization of neutron fields around high-energy X-ray radiotherapy machines. Radiation Protection Dosimetry. 2004;**110**:503-507. DOI: 10.1093/rpd/nch274

[47] ICRP Publication 103. The 2007 recommendations of the international commission on radiological protection. Annals of the ICRP. 2007;**37**(2-4):334

[48] Mesbahi A, Ghisai H, Mahdavi SR. Photoneutron and capture gamma dose equivalent for different room and maze layouts in radiation therapy. Radiation Protection Dosimetry. 2010;**140**(3):242-249. DOI: 10.1093/rpd/ncp303

- [49] ICRP Publication 26. Recommendations of the international commission on radiological protection. Annals of the ICRP. 1977;**1**(3):80
- [50] ICRP Publication 60. The 1990 recommendations of the international commission on radiological protection. Annals of the ICRP. 1991;**21**(1-3):202
- [51] International Commission on Radiation Units and Measurements. ICRU report 66, determination of operational dose equivalent quantities for neutrons. Journal of the ICRU. 2001;**1**(3):94
- [52] International Commission on Radiation Units and Measurements. ICRU report 85a, fundamental quantities and unit for ionizing radiation. Journal of the ICRU. 2011;**11**(11):33
- [53] ICRP Publication 74. Conversion coefficients for use in radiological protection against external radiation. Annals of the ICRP. 1996;**26**(3-4):205
- [54] ICRP 116. Conversion coefficients for radiological protection quantities for external radiation exposures. Annals of the ICRP. 2010;**40**(2-5):1-257. DOI: 10.1016/j.icrp.2011.10.001
- [55] ICRU Report 57. Conversion coefficients for use in radiological protection against external radiation. Journal of the ICRU. 1997
- [56] Rawool-Sullivan M, Sullivan J. Understanding Doppler Broadening of Gamma Rays [Report]. Los Alamos National Laboratory. 2014. DOI: LA-UR-14-23048
- [57] Thomadsen B, Ranvinder N, Bateman FB, Farr J, Glisson C, Islam M, et al. Potential hazard due to induced radioactivity secondary to radiotherapy: The report of task group 136 of the American Association of Physicists in Medicine. Health Physics. 2014;**107**(5):442-460. DOI: 10.1097/HP.0000000000000139
- [58] Schmidt FAR. The Attenuation Properties of Concrete for Shielding of Neutrons of Energy Less than 15 MeV. Oak Ridge, Tennessee, USA: Oak Ridge National Laboratory: ORNL-RSIC-26 UC-34 – Physics. 1970. p. 160
- [59] IAEA Safety Standards Series No. GSG-7. Occupational Radiation Protection—General Safety Guide. STI/PUB/1785. 2018. p. 360